Eurographics Workshop on Natural Phenomena (2006)
E. Galin, N. Chiba (Editors)

Simulating Caustics due to Liquid-Solid Interface Menisci

Eric Bourque Jean-François Dufort Michelle Laprade Pierre Poulin

Laboratoire d'Informatique Graphique (LIGUM)
Département d'Informatique et de Recherche Opérationnelle
Université de Montréal

Abstract

A solid partially immersed in a liquid creates a local deformation of the liquid surface at their interface. This deformation, called a meniscus, exhibits high curvature, and as such, produces very intriguing caustic patterns. However, this natural phenomena has been neglected in almost all previous liquid simulation techniques. We propose a complete solution to model and render meniscal illumination effects. First, we outline a physically-motivated approach to approximating the geometry of the meniscus. We then describe the targeted photon map, an adapted photon map which facilitates efficient sampling of the finely tessellated menisci. This technique, which integrates well within traditional photon mapping, allows for automatically rendering illumination effects for complex solid-liquid interfaces. Several images rendered using this technique are presented and are compared to their real-world counterparts.

Categories and Subject Descriptors (according to ACM CCS): I.3.7 [Computer Graphics]: Three-Dimensional Graphics and Realism

1. Introduction

There are many phenomena of striking beauty and complexity in nature. In particular, the interaction of light with matter has captivated both scientists and artists for centuries. One such phenomenon, referred to as a *caustic*, is due to a bundle of light rays which have been specularly reflected off or refracted through a curved surface. The word caustic means *to burn*, a fact to which many children who have played with a magnifying glass can attest. Caustics combine high intensities, fine details, as well as soft or sharp gradients into very intricate patterns of light.

Liquids provide a fertile ground for caustics. Rendering algorithms for simulating caustics have been extensively investigated in the field of computer graphics. For instance, fluid simulation is an active area of research, and high-quality rendering of the resulting animations involves simulating caustic patterns. Many approaches have thus been proposed to simulate these complex specular light paths.

Of particular interest is the narrow region at the interface between a liquid and a partially-immersed solid. This region, called the *meniscus*, exhibits high curvature due to intermolecular forces both within and between the liquid and the solid. This curved region of the liquid can focus light rays producing caustics on the intersecting solid as well as on the bottom of the liquid container.

This paper presents a complete solution to automatically model and render menisci and their lighting effects. First, in Sec. 2 we review the physical properties of the meniscus and in Sec. 3 we propose a method to geometrically model the meniscus shape at the interface between a liquid surface and a solid, where both are represented as polygonal tessellations. In Sec. 4, we outline our adapted photon map, the *targeted photon map*, which is sampled in 3D from the meniscus surface in order to better capture the desired caustic effects. Finally, we present results using our technique in Sec. 5, and revisit our contributions and outline future research directions in Sec. 6.

2. Background

All matter is made up of small particles which are constantly exerting forces on one another resulting in complex interactions. The effects we will discuss in this paper are di-

© The Eurographics Association 2006.

delivered by EUROGRAPHICS DIGITAL LIBRARY www.eg.org diglib.eg.org

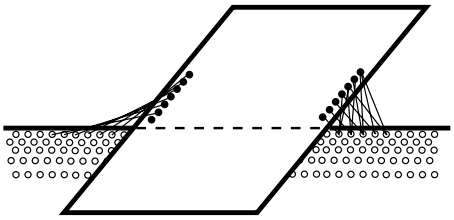

Figure 1: *The meniscus height is dependent on the solid-liquid contact angle. For an acute angle, there are more solid molecules in close proximity to the liquid molecules (right side). This results in a higher local attractive force which pulls the liquid higher than for an obtuse contact angle (left side).*

rectly related to these forces, particularly those between the molecules of a liquid and of a solid.

The attraction between the molecules of a liquid due to the inter-molecular forces creates a phenomenon known as surface tension. Within the liquid, individual molecules are pulled equally in all directions by their neighbouring molecules resulting in a uniform density. For very large bodies of liquid such as an ocean, the density actually increases slightly with depth due to the compression imposed by the weight of the water above. At the surface, however, the molecules are being pulled down by the deeper molecules, but there are no liquid molecules above pulling them up. This results in the liquid compressing at the top and forming a thin film which is more difficult to penetrate since the molecules are arranged in a locally higher density.

When a volume of liquid is in contact with a solid, there is a surface deformation along the intersection contour. The shape of this deformation, called a *meniscus*, is determined by the inter-molecular forces between the solid and the liquid. If the molecules comprising the intersecting solid attract the liquid molecules, then the liquid surface is pulled upwards around the solid creating a concave profile. Conversely, a convex profile is created if the solid's molecules repel the liquid molecules.

The height the meniscus climbs on the solid is dependent on the contact angle it forms with the liquid surface. For an acute contact angle, there are more solid molecules in close proximity to the liquid molecules. This results in a higher local attractive force which pulls the liquid higher than for an obtuse contact angle (see Fig. 1).

There is a common phenomenon, named the *shadow-sausage effect* by Adler [Adl67], which occurs when a cylindrical solid is partially immersed in a liquid. The cylinder casts a shadow on the ground of the container, but the shadow is negated by light refracted through the meniscus [Smi68, LAE*03]. This creates a shadow which resembles linked sausages as can be seen in Fig. 2.

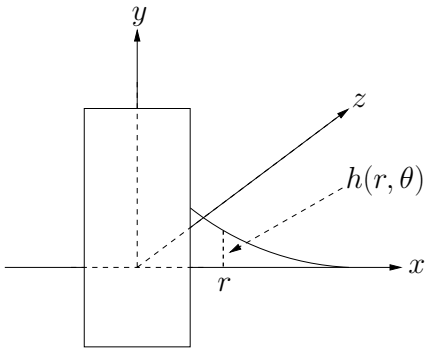

Figure 3: *The height of the meniscus around a cylinder whose axis passes through the origin can be described in polar coordinates by $h(r,\theta)$. The water is in the xz plane, and θ denotes the angle in that plane from the x axis.*

3. Modelling the Meniscus

Consider a cylinder whose axis passes through the origin as is shown in Fig. 3. The height h of the meniscus in polar coordinates, if the liquid surface is in the xz plane, can be described by the function $h(r,\theta)$ where $h \to 0$ as $r \to \infty$. Using the length scale $L \equiv (\gamma/\rho g)^{\frac{1}{2}}$ where γ, ρ, and g describe the liquid's surface tension, density, and the Earth's gravitational acceleration, and C is the mean curvature at any point on the liquid surface, then the function h satisfies the non-linear partial differential equation [HS69]

$$2C - h/L^2 = 0. \tag{1}$$

While this particular function can be approximated by rather complex numerical methods assuming the slope of the meniscus is small everywhere [BH83], it unfortunately does not generalise to arbitrary intersection contours. Given the ubiquity of polygonal representations in computer graphics, particularly in liquid simulations, it is desirable to provide reasonable approximations for menisci between polygonised liquid surfaces and solids.

Watt presented an example of manually modelling the meniscus for a cylindrical solid using the interpolated normals of an elliptical annulus [Wat90]. We seek a technique which is able to handle arbitrary solid intersections, and which can generate the associated menisci automatically.

3.1. Meniscus Contour

In order to create a triangle mesh approximation to the meniscus geometry, we must initially identify solids which may intersect the liquid surfaces in the scene. This is easily accomplished by hierarchically checking for overlapping bounding boxes between liquid and solid elements in the scene. We then wish to determine the contours of all of the liquid-solid intersections.

© The Eurographics Association 2006.

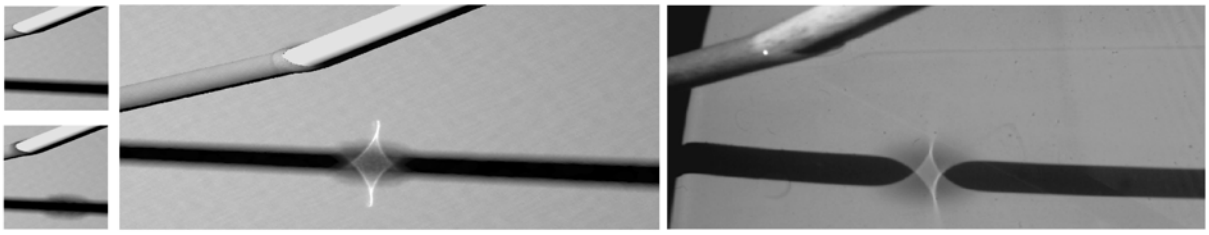

Figure 2: *The shadow-sausage effect. The top-left image was rendered without caustics or meniscus geometry using PBRT [PH04], the bottom-left was rendered with caustics and the automatically modelled meniscus geometry using PBRT, the middle image was rendered using the method described in this paper, and the image on the right is a real photo of the effect (image originally appeared as Fig.1(b) in [LAE*03]). Notice how the meniscus geometry is under-sampled using a traditional photon mapping technique (bottom-left).*

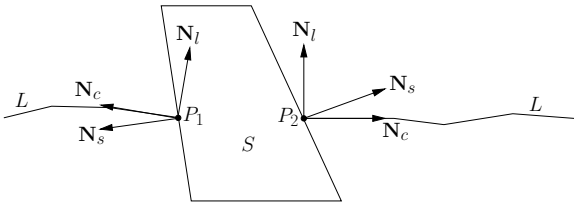

Figure 4: *The normals for two intersection points P_1 and P_2 between a solid S and a liquid L . $\mathbf{N}_l$ and $\mathbf{N}_s$ denote the interpolated liquid and solid normals at the point of intersection. $\mathbf{N}_c$ is the contour normal which is $\mathbf{N}_s$ projected onto the liquid triangle associated with the intersection.*

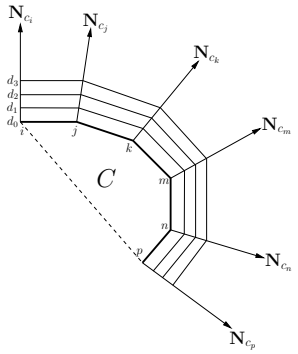

Figure 5: *The contour polyline C and the polylines propagated along the contour normals $\mathbf{N}_c$ for increasing values of d as seen from above.*

To compute the contours, we first perform intersection tests on the triangles comprising both the solid and liquid objects using Möller's fast triangle-triangle intersection technique [Mö97]. Each intersecting triangle-pair produces a line segment whose end-points have two normals each: interpolated normals from the liquid surface ($\mathbf{N}_l$) and from the solid ($\mathbf{N}_s$) as shown in Fig. 4. If the solid does not have interpolated normals, such as for a cube, the solid-liquid intersection for adjacent solid polygonal faces will produce two vertices at the same location, but with different solid normals. Vertices with a multiplicity of 2 are specially marked as *joint vertices*.

The resulting intersection segments are assembled into polygonal chains. These chains are then formed into contours; that is, a collection of ordered vertices with associated normals. The contour normal $\mathbf{N}_c$ is computed by projecting the solid normal $\mathbf{N}_s$ onto the liquid triangle associated with each contour point. The contours are checked to ensure they are not degenerate (e.g., duplicate points not labelled as joint vertices, closeness constraints, or self-intersections), and are optionally refined by adding more sample points along the intersection segments.

3.2. Meniscus Profile

We seek a meniscus height approximation function which is simple to compute, is continuous, has a well-defined extent, and is roughly similar in shape to the solution to Eq. (1). In addition, the height approximation function should not be restricted to cylindrical intersections, but should be applicable to arbitrary non-intersecting contours. As such, our height function is not parameterised in polar coordinates, but is instead evaluated radially at regular steps d along the contour normals $\mathbf{N}_c$ as shown in Fig. 5. For a given propagated contour polyline at a distance $d \in [0,1]$ along $\mathbf{N}_c$, each vertex is displaced by $h(d,\alpha)$ along $\mathbf{N}_l$ where α is the contact angle between the solid and the liquid at the contour point. The height function used for the results presented in this paper is

$$h(d,\alpha) = \left(\frac{-2L}{\pi}\alpha + 2L\right)\left(1 - \sin\left(\frac{d\pi}{2}\right)\right) \qquad (2)$$

where L is the length scale of the liquid. This gives a continuous decreasing function whose height and curvature vary with the contact angle α. Our technique supports liquids

© The Eurographics Association 2006.

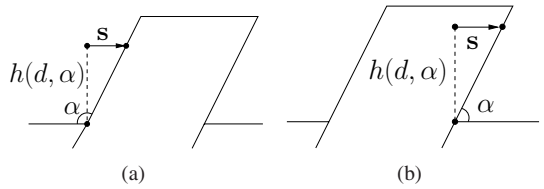

Figure 6: *Displacing a point at the height h of the meniscus by* **s** *so that it bonds to the solid, for obtuse and acute contact angles* α.

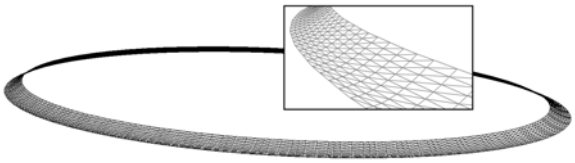

Figure 7: *A closeup view of a small section of an automatically created meniscus triangle mesh.*

which are not flat, as long they are locally smooth at the scale of the meniscus.

The propagation from joint vertices is treated similarly to other polyline vertices, except more interpolated directions $\mathbf{N}_c$ might be required when the two original $\mathbf{N}_c$'s form too large an angle.

As mentioned above, when the immersed solid is not perpendicular to the liquid surface, the height of the meniscus changes according to the contact angle α. Since raising the contour point to the correct height will, in general, not touch the intersecting solid, we need to compute a displacement vector **s** to ensure that the meniscus bonds to the solid (see Fig. 6).

Although an analytic geometrical solution exists to calculate the displacement, it is not always appropriate because it is possible that the displaced point will lie on a different triangle in the solid's tessellation. To alleviate this problem, we instead use ray intersection tests to compute the displacement vector which produces a tight fit to the intersecting solid. The displacement associated with the individual contour points is then propagated along each contour polyline for the corresponding vertex. Note that it is possible that this displacement can slightly change the meniscus shape locally, however, this is generally imperceptible in the final image due to the scale of the meniscus.

The points generated by this modelling process are then assembled into a triangle mesh (see Fig. 7), and these triangles are labelled as *targets* for rendering. The calculation of the menisci contribute negligibly to the total rendering time (an average of 0.284% of the total rendering time for the images in this paper).

Unfortunately, for very large obtuse contact angles, it is still possible that displacing the meniscus to ensure contact with the solid could cause the meniscus itself to briefly intersect the solid. While this is not necessarily significant at the scale of the meniscus, our system allows the user to instead choose to have the meniscus projected onto the liquid surface, preserving the normals from the original displaced mesh. This option produces a similar caustic pattern discussed later (see Fig. 13). In addition, our technique does not handle intersections between menisci as might happen when two solids are immersed in a liquid very close to each other.

Finally, there are user parameters which provide a fine level of control over the generated menisci. These include scale factors for both the height and sweep length of the generated menisci, whether the meniscus should be represented as a curved or a flat surface, as well as several meniscus profile generating functions. These allow a graphic artist to accentuate or diminish lighting effects according to the image he is trying to convey [PVL*05].

4. Rendering

The addition of a meniscus to the scene geometry leads to three possible illumination changes:

1. thin, bright highlights present on the meniscus itself;
2. caustics cast directly on the intersecting solid;
3. caustics cast on other surfaces present in the scene.

We describe our approach to rendering these effects below.

4.1. Direct Illumination

Typically, the meniscus is much smaller than the other objects in the scene, leading to a very fine mesh representation. The specular property of most liquids, combined with the high curvature of the meniscus, produces very thin and bright highlights which are prone to aliasing.

Tanaka and Takahashi [TT91] derived an analytical formulation for a similar situation which occurs along thin rounded edges of polygonal models. Their Phong-like reflection model calculates the projected pixel areas of each polygon, and then analytically computes the final contribution based on the variation of normals within these areas.

In order to allow any type of reflection model, we rely instead on sampling the normals within the estimated projected pixel area: for any direct or indirect path along an eye ray which intersects the meniscus, we select the polygons of the meniscus within a given radius of the intersection. We then compute the shading at this intersection by averaging the shading resulting from normals at *n* randomly sampled points within the selected polygons. The differential ray mechanism [Ige99] provided in the rendering algo-

© The Eurographics Association 2006.

rithm [PH04] determines an appropriate radius based on the associated pixel size.

4.2. Indirect Illumination

Caustics are formed when light is specularly reflected or refracted one or more times before hitting a non-specular surface, and are therefore only captured by indirect illumination solutions. The desire to simulate caustics has spawned an active field of research in computer graphics. Many rendering algorithms have thus been developed to respond to the highly directional behaviour of caustics, some of which will be outlined below. Unfortunately, the scale of the menisci challenges these approaches, most often preventing an adequate computation of the indirect illumination.

Monte Carlo path tracing is a traditional technique used to simulate a scene's indirect illumination by following ray paths from the camera through the scene and ultimately to the light sources [Kaj86]. The concept of emitting photons from the light sources and following their interactions with elements in the scene has enabled simulating the indirect illumination for arbitrarily complex scenes [Col94, JC95, SWH*95, WHSG97]. Unfortunately, in our case, the probability of intersecting the fine mesh representing the meniscus is so low that rendering its effects suffers from very slow convergence or under-sampling artifacts (see Fig. 2). We resolve this sampling issue by identifying the meniscus geometry and labelling it for special treatment as described below.

Watt gives an example of simulating the indirect illumination due to a manually-modelled meniscus [Wat90]. His approach projects each meniscus triangle from a point light source onto the receiving triangles in the scene, and the irradiance is estimated by the area ratios of specular-receiving triangle-pairs. While all meniscus contributions are treated, this technique requires scan-conversion of the meniscus triangles onto a general 3D scene, which is difficult to achieve robustly.

Mitchell and Hanrahan [MH92] have introduced an optimisation technique that identifies the extremal paths (caustics) from reflective surfaces given a point light source and a point to shade. Although their technique could be applied to handle caustics due to a meniscus, the computation must be performed for all visible points in a scene, and as such it does not scale well when the menisci grow in number and complexity. Moreover, the techniques by Watt and by Mitchell and Hanrahan are difficult to adapt to efficiently support illumination from extended lights.

Other, more general rendering techniques might handle meniscus caustics efficiently. For instance, bidirectional techniques [LW93, VG94], and in particular a variation of Metropolis [VG97] optimised for these light-meniscus-surface paths, might prove to be quite efficient. However they require fine tuning of path perturbations, which can be difficult where scene and light source configurations are complex. While the results could be roughly equivalent using a Metropolis-based solution, we have instead opted to use the more common photon mapping rendering algorithm.

Photon mapping is particularly well-suited to simulating caustics [Jen96], thanks to its caustic map and projection map. The latter, a projection of the scene onto a central point on a light source, helps determine where in the scene photons should be emitted in order to intersect particular scene geometry. Given that light sources can have different types, shapes and sizes, and that a projection map relies on projected specular surfaces, it is not clear how well meniscal caustics can be simulated using traditional photon mapping alone. Nevertheless, our solution draws from these two specialised maps and other mechanisms developed within the photon mapping framework.

Other techniques have concentrated on specially labelled specular surfaces in order to render caustics in real time for interactive systems. These techniques frequently rely on graphics hardware and texture look-ups [TS00, WS03], or distributing the rendering over multiple CPUs [GWS04]. Integration of these techniques in generic rendering algorithms remains an issue.

4.2.1. Targeting Photons

The popularity of photon mapping [Jen01] and the availability of efficient and documented implementations [PH04] make it an attractive framework for rendering meniscal caustics. However, randomly sampling a projection map [JC95] from a point on a light source is not as efficient when the meniscus geometry covers only a small fraction of each identified projection map pixel. Moreover, as the light source gets larger, the central point of a projection map will not guarantee a good sampling of the meniscus geometry for the caustic and global photon maps. We have instead devised an additional photon map, the *targeted photon map*, which captures the indirect illumination attributed to the meniscus. The use of an additional photon map provides finer control over the meniscal caustics in the final rendering since these are a result of specific light paths.

To add a photon in the targeted photon map, we first initiate a sample point p with normal $\mathbf{p}_N$ directly on the meniscus geometry using a uniform distribution weighted by the area of the triangles in the tessellation of the meniscus.

For each photon, a *light sample* point l is chosen on a randomly selected light source. This source is chosen by importance sampling based on the area and the power of each light source in the scene, as is conventionally done when using a particle tracing approach.

To eliminate photons with a low contribution, we perform Russian roulette based on the cosine factor determined by $\mathbf{p}_N$ and the light vector $\mathbf{L} = l - p/||l - p||$. This allows the same power to be assigned to all photons emitted from a given light source, since fewer photons will be kept for larger

© The Eurographics Association 2006.

angles between $\mathbf{L}$ and $\mathbf{p}_N$ at p. The visibility between p and l is then computed, and the current photon is discarded if the light sample is not visible. If the photon initiated at p is retained, its power is set according to the light source's probability distribution function at the light sample l in the direction $-\mathbf{L}$.

The photon is then traced similarly to regular photon mapping, undergoing reflections and refractions, and is stored in the targeted photon map if it intersects a surface considered diffuse by Russian roulette selection, according to the reflectance types of the surface material. Our use of an additional photon map allows fine tuning of the contribution of the targeted photons in the density estimation used when computing the radiance estimate. This also provides control over the bias introduced by the non-uniformity of the targeted photons with respect to the entire scene. In the rare case that a regular photon hits a meniscus directly from the light source, it is eliminated since we assume that our sampling scheme has already captured its contribution.

5. Results

The images in this paper are computed in high dynamic range and encoded in the EXR format. They have all been tone mapped using Ward's contrast-based tone map operator [War94].

The two images in Fig. 8 show a real teapot partially immersed in water and its synthetic counterpart rendered using automatically generated menisci. The real teapot is 7cm long and is made of a semi-rough metal. At this size, water surface tension perturbs the shape of the menisci near the interfaces which is clearly visible from the highlights. These small geometric details have not been modelled, the light has only been roughly estimated, and direct rendering of water mirror reflection has been omitted. Despite these approximations, one can observe the similarity of the intriguing caustics and shadows produced by the handle and the spout.

In Fig. 9, a paperclip floats on water. It produces interesting elongated caustics. The internal curve of the paperclip is not touching the water, thus casting a soft shadow but not contributing any caustic.

Even for tiny floating objects, such as hair, caustics due to the menisci are quite striking. Figure 10 shows caustics from a real hair next to our simulated meniscal caustics. As both hairs curl, they do not touch the water along their entire length, alternating between areas of caustics and shadows.

In Fig. 11, we demonstrate the generic nature of our system with a collection of arbitrary objects partially immersed in, and floating on the water. We see caustics resulting from the vase, the spider, the heart, the bird, and the handle of the umbrella, and we see the highlights from the menisci where the water contacts the walls. Note that some of the caustic patterns are repeated in different locations since this scene has multiple light sources.

(a)

(b)

Figure 8: *(a) Real and (b) synthetic teapots partially immersed in water. Observe the similar caustics caused by the handle and the spout.*

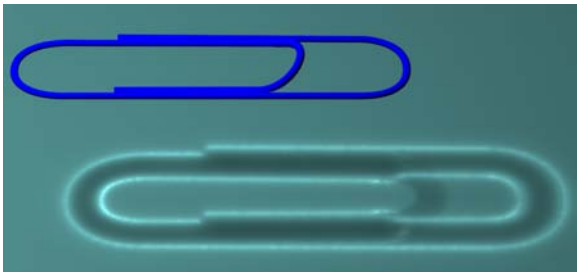

Figure 9: *A floating paperclip produces elongated caustics.*

The real shape of the meniscus profile is still not completely understood, and sophisticated approximations are valid only for simple shapes, such as a cylindrical object. It appears that the shape of the caustics is mainly captured by the contour shape of the meniscus. Surprisingly, the meniscus profile does not have as much impact on the overall shape of the resulting caustics, but does exhibit a minor influence on the gradient of light within the caustics. To support this observation, we investigated a number of different profile functions, a few of which are illustrated in Fig. 12.

Figure 13 shows two caustics produced by the same meniscus triangles, except in (b) the triangles have been flat-

© The Eurographics Association 2006.

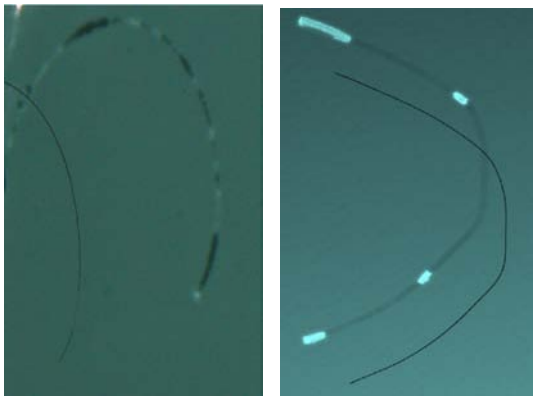

(a) (b)

Figure 10: *A real hair floating on water (a), and simulated hair floating on water (b). Note that the hair does not completely touch the water in either image, producing bright caustics where it does touch.*

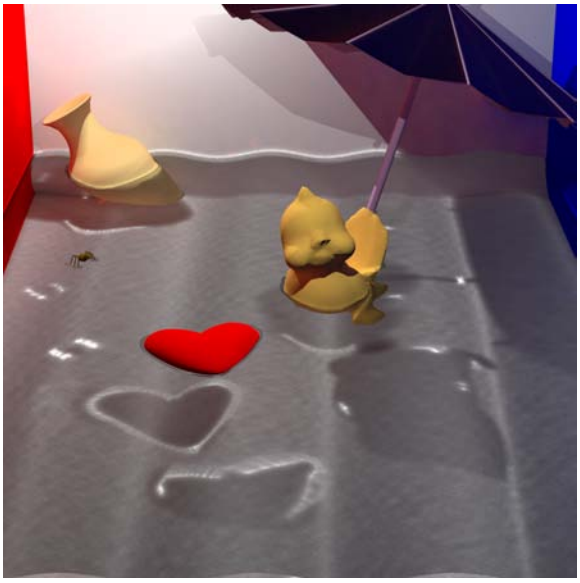

Figure 11: *A scene containing multiple light sources and multiple objects partially immersed and floating on slightly wavy water.*

tened onto the liquid surface, while preserving their original surface normals. The subtle differences, shown as a difference of tone mapped images in Fig. 13(c), appear more like noise.

6. Discussion

The meniscus at the interface of a solid partially immersed in a liquid produces very interesting caustics and elongated

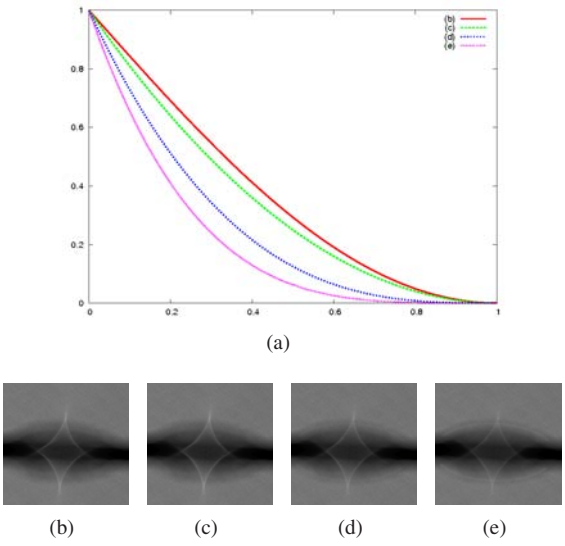

(a)

(b) (c) (d) (e)

Figure 12: *Four functions approximating the meniscus profile, and their corresponding images. Note that the negligible differences in the caustics are mainly gradient variations.*

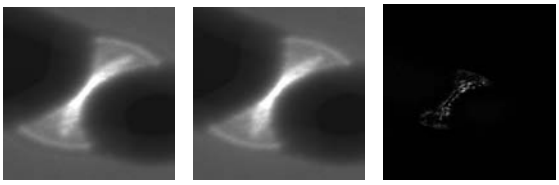

(a) (b) (c)

Figure 13: *Meniscus geometry projected onto the liquid triangles. The original produces the caustic shown in (a), and the version with preserved normals produces the caustic shown in (b). The difference between the images is shown in (c).*

highlights, both of which are particularly challenging to reproduce efficiently with traditional modelling and rendering algorithms.

In this paper, we have presented a complete solution to the simulation of the lighting effects due to arbitrary liquid-solid interface menisci. A geometrical representation of the meniscus shape is efficiently and robustly extracted by hierarchically intersecting solid and liquid triangular meshes, and linking the oriented segments into closed contours.

We have shown that obtaining the correct intersection contour is critical to achieving the desired caustic patterns, while the profile of the meniscus is less significant.

Direct illumination challenges are answered by an adapted local shading based on sampling with differential rays, and indirect illumination is captured by a targeted pho-

© The Eurographics Association 2006.

ton map initiated with an importance distribution of photons directly over the meniscus meshes. These solutions have been integrated within a publicly available photon mapping rendering system [PH04].

While our approach provides visually satisfying results, a more comprehensive solution for robustly calculating the meniscus geometry displacement in the presence of large obtuse contact angles would be of interest. Other extremely thin phenomena, such as air bubbles and soap film could possibly be simulated using a similar framework. Finally, it could be interesting to extract meniscal geometry and profiles directly from photos, hopefully resulting in a better understanding and parametrisation of surface tension.

Acknowledgements

The authors wish to thank NSERC and FQRNT for their financial support. Simon Bouvier-Zappa and Yann Rousseau assisted in the preparation of the paper. Finally, we would like to thank the reviewers for their valuable comments on this research.

References

[Adl67] ADLER C.: Shadow-sausage effect. *American Journal of Physics 35* (1967), 774–776.

[BH83] BERRY M. V., HAJNAL J. V.: The shadows of floating objects and dissipating vortices. *Journal of Modern Optics 30*, 1 (1983), 23–40.

[Col94] COLLINS S.: Adaptive splatting for specular to diffuse light transport. In *Eurographics Workshop on Rendering* (1994), pp. 119–135.

[GWS04] GÜNTHER J., WALD I., SLUSALLEK P.: Real-time caustics using distributed photon mapping. In *Eurographics Workshop on Rendering* (2004), pp. 111–122.

[HS69] HUH C., SCRIVEN L.: Shapes of axisymmetric fluid interfaces of unbound extent. *Journal of Colloid and Interface Science 30*, 3 (1969), 323–337.

[Ige99] IGEHY H.: Tracing ray differentials. In *Proceedings of SIGGRAPH 99* (1999), pp. 179–186.

[JC95] JENSEN H. W., CHRISTENSEN N. J.: Photon maps in bidirectional Monte Carlo ray tracing of complex objects. *Computers & Graphics 19*, 2 (March 1995), 215–224.

[Jen96] JENSEN H. W.: Global illumination using photon maps. In *Eurographics Workshop on Rendering* (1996), pp. 21–30.

[Jen01] JENSEN H. W.: *Realistic Image Synthesis Using Photon Mapping*. AK Peters, 2001.

[Kaj86] KAJIYA J. T.: The rendering equation. In *Proceedings of SIGGRAPH 86* (1986), vol. 20, pp. 143–150.

[LAE*03] LOCK J. A., ADLER C. L., EKELMAN D., MULHOLLAND J., KEATING B.: Analysis of the shadow-sausage effect caustic. *Applied Optics 42*, 3 (2003), 418–428.

[LW93] LAFORTUNE E. P., WILLEMS Y. D.: Bi-directional path tracing. In *Compugraphics 93* (1993), pp. 95–104.

[MH92] MITCHELL D. P., HANRAHAN P.: Illumination from curved reflectors. In *Proceedings of SIGGRAPH 92* (1992), vol. 26, pp. 283–291.

[Mö97] MÖLLER T.: A fast triangle-triangle intersection test. *Journal of Graphic Tools 2*, 2 (1997), 25–30.

[PH04] PHARR M., HUMPHREYS G.: *Physically Based Rendering From Theory to Implementation*. Morgan Kaufmann, 2004.

[PVL*05] PELLACINI F., VIDIMCE K., LEFOHN A., MOHR A., LEONE M., WARREN J.: Lpics: a hybrid hardware-accelerated relighting engine for computer cinematography. *ACM Transactions on Graphics 24*, 3 (2005), 464–470.

[Smi68] SMITH M. J.: Comment on: Shadow-sausage effect. *American Journal of Physics 36* (1968), 912–914.

[SWH*95] SHIRLEY P., WADE B., HUBBARD P., ZARESKI D., WALTER B., GREENBERG D. P.: Global illumination via density estimation. In *Eurographics Workshop on Rendering* (1995), pp. 219–231.

[TS00] TRENDALL C., STEWART A. J.: General calculations using graphics hardware with applications to interactive caustics. In *Eurographics Workshop on Rendering* (2000), pp. 287–298.

[TT91] TANAKA T., TAKAHASHI T.: Precise rendering method for edge highlighting. In *Proceedings of CG International 91* (1991), pp. 283–298.

[VG94] VEACH E., GUIBAS L.: Bidirectional estimators for light transport. In *Eurographics Workshop on Rendering* (1994), pp. 147–162.

[VG97] VEACH E., GUIBAS L. J.: Metropolis light transport. In *Proceedings of SIGGRAPH 97* (1997), pp. 65–76.

[War94] WARD G.: *Graphics Gems IV*. Academic Press, 1994, ch. A contrast-based scalefactor for luminance display, pp. 415–421.

[Wat90] WATT M.: Light-water interaction using backward beam tracing. In *Proceedings of SIGGRAPH 90* (1990), pp. 377–385.

[WHSG97] WALTER B., HUBBARD P. M., SHIRLEY P., GREENBERG D. F.: Global illumination using local linear density estimation. *ACM Transactions on Graphics 16*, 3 (1997), 217–259.

[WS03] WAND M., STRASSER W.: Real-time caustics. *Computer Graphics Forum 22*, 3 (2003), 611–620.

© The Eurographics Association 2006.